Characteristics of Land–Atmosphere Interaction Parameters over the Tibetan Plateau

SHUZHOU WANG

Institute of Tibetan Plateau Research, and Institute of Atmospheric Physics, Chinese Academy of Sciences, Beijing, China

YAOMING MA

Key Laboratory of Tibetan Environment Changes and Land Surface Processes, Institute of Tibetan Plateau Research, Chinese Academy of Sciences, Beijing, China

(Manuscript received 20 January 2010, in final form 4 November 2010)

ABSTRACT

In this study, eddy covariance flux data collected from three research stations on the Tibetan Plateau—Qomolangma for Atmospheric and Environmental Observation and Research, Nam Co for Multisphere Observation and Research, and Southeast Tibet Station for Alpine Environment Observation and Research, Chinese Academy of Sciences—are used to analyze the variation of momentum transfer coefficient (C_D), heat transfer coefficient (C_H), aerodynamic roughness length (z_{0m}), thermal roughness length (z_{0h}), and excess resistance to heat transfer (kB^{-1}, where k is von Kármán's constant and B^{-1} is a non-dimensional bulk parameter). The following results are found. The monthly average surface roughness, bulk transfer coefficient, and excess resistance to heat transfer at all three stations are obtained. The values of average heat bulk transfer coefficients are larger than those of average momentum bulk transfer coefficients at all three stations. The parameter kB^{-1} exhibits clear diurnal variations with lower values in the night and higher values in the daytime, especially in the afternoon. Negative values of kB^{-1} are often observed in the night for relatively smooth surfaces on the Tibetan Plateau, indicating that heat transfer efficiency may exceed that of momentum transfer.

1. Introduction

As the largest and highest plateau in the world, the Tibetan Plateau affects the general circulation of the atmosphere and plays a very important role in the Asian monsoon system. The land–atmosphere interactions not only affect the development of the local atmospheric boundary layer, but also change the horizontal gradient of temperature and moisture at a continent scale (Yang et al. 2003). What is more, the land surface heterogeneity leads to differences in the surface roughness, bulk transfer coefficient, and excess resistance to heat transfer over the different land surfaces on the Tibetan Plateau (Ma et al. 2008). Thus, an observational analysis of land–atmosphere interaction parameters in different landscapes of the Tibetan Plateau is of great significance. Some interesting detailed studies concerning these key parameters have been reported (e.g., Miao et al. 1998; Li et al. 2001, 2002; Li and Tao 2005; Ma et al. 2002; Yang et al. 2003, 2008) during the past few years. However, most of these studies used AWS data without using eddy covariance flux data for a whole year.

In this study, eddy covariance flux data collected from three research stations on the Tibetan Plateau—Qomolangma for Atmospheric and Environmental Observation and Research (hereafter Qomolangma), Nam Co for Multisphere Observation and Research (hereafter Nam Co), and Southeast Tibet Station for Alpine Environment Observation and Research (hereafter Southeast Tibet station), Chinese Academy of Sciences—are used to analyze the variation of momentum transfer coefficient (C_D), heat transfer coefficient (C_H), aerodynamic roughness length (z_{0m}), thermal roughness length (z_{0h}), and excess resistance to heat transfer (kB^{-1}, where k is von Kármán's constant and B^{-1} is a non-dimensional bulk parameter). The purpose of this paper is to present the characteristics of these key parameters over different

Corresponding author address: Dr. Yaoming Ma, Institute of Tibetan Plateau Research, Chinese Academy of Sciences, P.O. Box 2871, Beijing 100085, China.
E-mail: ymma@itpcas.ac.cn

DOI: 10.1175/2010JHM1275.1

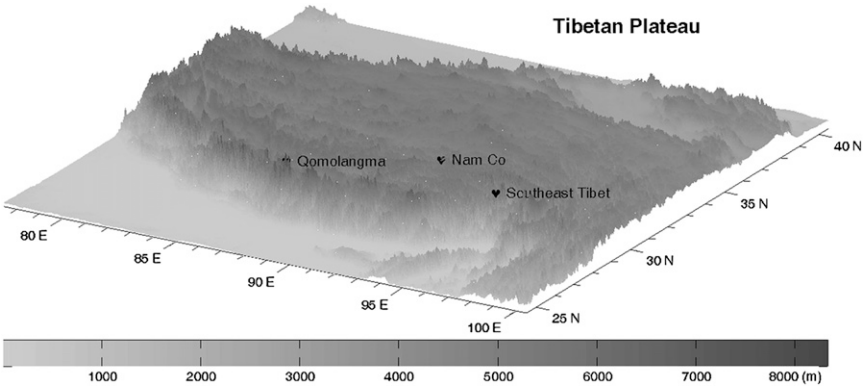

FIG. 1. The location of the three stations on the Tibetan Plateau used in this study.

landscapes of the Tibetan Plateau for the whole year of 2007.

2. Data

Data used in this paper were collected from three research stations on the Tibetan Plateau: Qomolangma, Nam Co, and Southeast Tibet. All three stations (Fig. 1 shows their location) are established by the Institute of Tibetan Plateau Research, Chinese Academy of Sciences. Qomolangma (28°13′N, 86°34′E, 4276 m MSL) is located on the northern slope of Mt. Qomolangma (Mt. Everest). The surface of the site is covered by sandy soil with small rocks. Nam Co (30°46′N, 90°59′E, 4730 m MSL) is located at the southeast shore of Nam Co Lake, on the northern slope of the Nyainqentanglha Mountains. The site has a relatively smooth surface and is covered by very sparse and short grasses in the monsoon season. Southeast Tibet station (29°46′N, 94°44′E, 3230 m MSL) is located on the southeast Tibetan Plateau. The site's surface is covered with dense canopy, and the site is surrounded by forest. We collected data from these stations for the whole year of 2007 (there is no data collected at Nam Co in May and July of 2007). Eddy fluxes were measured with an eddy covariance system consisting of an open-path infrared CO_2/H_2O gas analyzer (LI-7500, LI-COR Inc.) and a 3D sonic anemometer (CSAT3, Campbell Scientific Inc.) at a height of 3 m above ground level and the data average recording interval was set to 30 min at Qomolangma and Nam Co, while data from Southeast Tibet station was measured with 10-min averaging. All data collected were corrected for coordinate rotation (Kaimal and Finnigan 1994; Wilczak et al. 2001), Webb-Pearman-Leuning (WPL) correction (Webb et al. 1980), and sonic temperature correction. As a feasible method for coordinate rotation, the planar fit method (Wilczak et al. 2001) was used in this study.

3. Methodology

a. Determination of surface roughness length

From the Monin–Obukhov similarity theory, the dimensionless wind shear and temperature gradient in a horizontally homogeneous surface layer are usually expressed as (Yang et al. 2002)

$$\frac{kz}{u_*}\frac{\partial U}{\partial z} = \varphi_m(\zeta) \quad \text{and} \tag{1}$$

$$\frac{kz}{T_*}\frac{\partial T}{\partial z} = \varphi_m(\zeta), \tag{2}$$

where U (m s^{-1}) is wind speed, T (K) is temperature, u_* (m s^{-1}) is friction velocity, T_* (K) is temperature scale (or friction temperature), ζ is stability parameter, and

TABLE 1. Flux parameterization schemes for kB^{-1}. The Prandtl number Pr = 0.71, $k = 0.4$, ν is the fluid kinematical viscosity, $\alpha = 0.52$, $\beta = 7.2$, and $\mathrm{Re}_* = z_{0m}u_*/\nu$.

Formula	Reference	Abbreviation
$kB^{-1} = \ln(\mathrm{Pr} \times \mathrm{Re}_*)$	Sheppard (1958)	S58
$kB^{-1} = k\alpha(8\mathrm{Re}_*)^{0.45}\mathrm{Pr}^{0.8}$	Owen and Thomson (1963)	O63
$kB^{-1} = 2.46\mathrm{Re}_*^{0.25} - 2$	Brutsaert (1982)	B82
$kB^{-1} = k\alpha\mathrm{Re}_*^{0.45}$	Zeng and Dickinson (1998)	Z98
$kB^{-1} = 1.29\mathrm{Re}_*^{0.25} - 2$	Kanda et al. (2007)	K07
$z_{0h} = (70\nu/u_*) \times \exp(-\beta u_*^{0.5}\lvert T_*\rvert^{0.25})$	Yang et al. (2007)	Y07

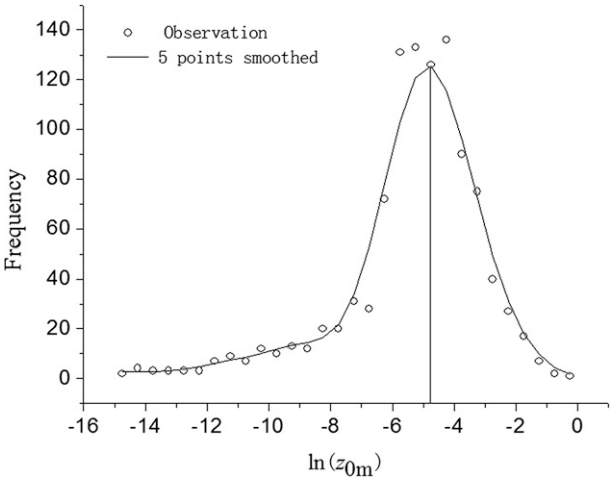

FIG. 2. Frequency distribution of $\ln(z_{0m})$ at Nam Co in October.

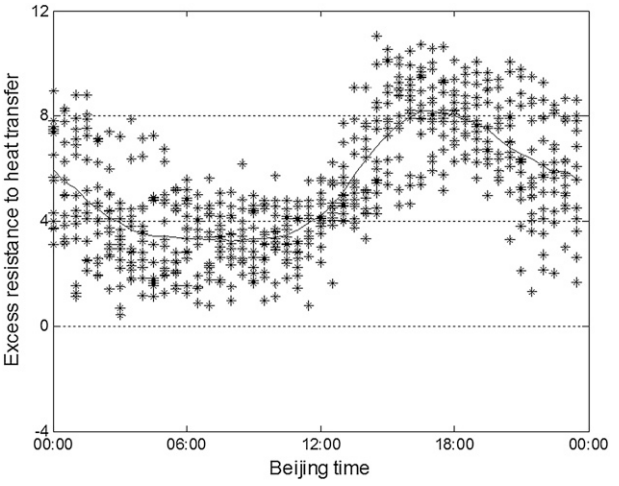

FIG. 3. The diurnal variations of observed kB^{-1} at Qomolangma in March (solid line is obtained by 5-point smoothing).

z is the height above the zero-plane displacement. The quantity φ_m is the stability function for momentum, and φ_h is the stability function for heat. The k is von Kármán's constant.

The equations above can be integrated from the roughness height level to the reference level (z), which results in (Yang et al. 2001)

$$U = \frac{u_*}{k}\left[\ln\left(\frac{z}{z_{0m}}\right) - \psi_m(\zeta,\zeta_m)\right] \quad \text{and} \tag{3}$$

$$T_s - T_a = \Pr\frac{T_*}{k}\left[\ln\left(\frac{z}{z_{0h}}\right) - \psi_h(\zeta,\zeta_h)\right], \tag{4}$$

where T_s is the surface temperature, T_a is the air temperature, $\zeta \equiv z/Lz$ is the height above the zero-plane displacement, L is Monin–Obukhov length, z_{0m} is the aerodynamic roughness length, and z_{0h} is the thermal roughness length. We have ζ_m $(=z_{0m}/L)$ as the stability function for momentum, and ζ_h $(=z_{0h}/L)$ as the stability function for heat. The quantity Pr is Prandtl number (=1 if $z/L \geq 0$ and 0.95 if $z/L < 0$). The term ψ_m is the integrated form of the stability function for momentum, and ψ_h is the integrated form of the stability function for heat.

Following the universal functions in Högström (1996) and the mathematical form of the correction terms in Paulson (1970), for stable surface layers, we obtain

$$\psi_m\left(\frac{z_{0m}}{L}, \frac{z}{L}\right) = -5.3(z - z_{0m})/L \quad \text{and} \tag{5}$$

$$\psi_h\left(\frac{z_{0h}}{L}, \frac{z}{L}\right) = -8.0(z - z_{0h})/L; \tag{6}$$

for unstable surface layers,

$$\psi_m\left(\frac{z_{0m}}{L}, \frac{z}{L}\right) = 2\ln\left(\frac{1+x}{1+x_0}\right) + \ln\left(\frac{1+x^2}{1+x_0^2}\right) - 2tg^{-1}x + 2tg^{-1}x_0 \quad \text{and} \tag{7}$$

$$\psi_h\left(\frac{z_{0m}}{L}, \frac{z}{L}\right) = 2\ln\left(\frac{1+y}{1+y_0}\right), \tag{8}$$

where $x = [1 - (19z/L)]^{1/4}$, $x_0 = [1 - (19z_{0m}/L)]^{1/4}$, $y = [1 - (11.6z/L)]^{1/2}$, and $y_0 = [1 - (11.6z_{0h}/L)]^{1/2}$.

The logarithmic wind profile can be rewritten from Eq. (3) as

$$\ln z_{0m} = \ln z - \psi_m\left(\frac{z_{0m}}{L}, \frac{z}{L}\right) - kU/u_*. \tag{9}$$

Given all the observed u_* and wind speed U, a set of $\ln(z_{0m})$ can be generated, and thus aerodynamic roughness length can be obtained. For an average value of roughness length, a method developed by Yang et al. (2008) can be applied, as the optimal value of z_{0m} would correspond to the peak frequency in the histogram of

TABLE 2. Average aerodynamic roughness (cm) of the three stations: Qomolangma (Qomo.), Nam Co, and Southeast Tibet (South. T.).

Station	Jan	Feb	Mar	Apr	May	Jun	Jul	Aug	Sep	Oct	Nov	Dec
Qomo.	2.40	2.99	3.34	3.02	3.47	2.47	2.24	2.02	2.24	2.82	2.24	2.28
Nam Co	1.66	1.83	1.85	2.23	—	2.87	—	1.83	0.86	0.84	0.87	0.89
South. T.	5.73	5.96	6.79	17.4	47.2	37.5	26.7	18.3	17.5	25.2	30.1	34.9

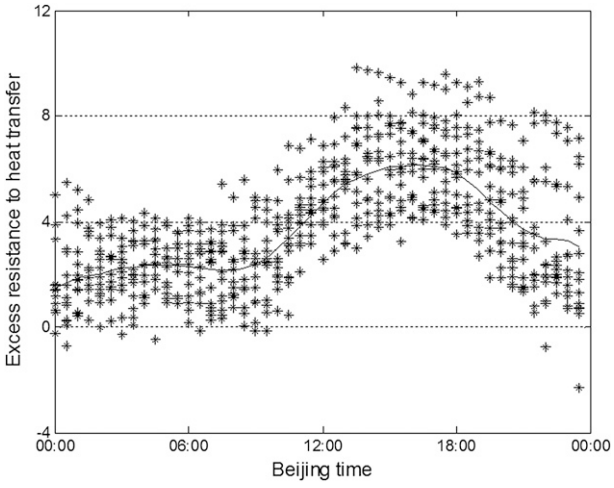

FIG. 4. As in Fig. 3, but for Nam Co.

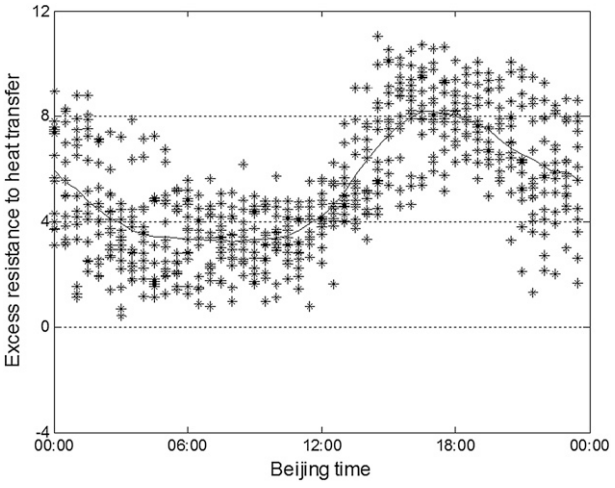

FIG. 5. As in Fig. 3, but for the Southeast Tibet station.

$\ln(z_{0m})$. It is generally accepted that z_{0h} is different from z_{0m} (e.g., Beljaars and Holtslag 1991), which can be derived from some kB^{-1} schemes shown in Table 1; we chose the Y07 parameterization scheme in this study.

b. Determination of excess resistance to heat transfer

The excess resistance to heat transfer kB^{-1} is used to parameterize the sensible heat exchange between the land surface and atmosphere. In past decades, the parameterization of kB^{-1} has attracted a number of theoretical and experimental studies (e.g., Garratt and Francey 1978; Brutsaert 1982; Verhoef et al. 1997; Ma et al. 2002; Yang et al. 2003, 2007, 2008; Kanda et al. 2007). It appears as a variable in many numerical models and satellite remote sensing parameterization methods, and we simply computed kB^{-1} using the z_{0m} obtained by the above-mentioned method with the following equation (Owen and Thomson 1963):

$$kB^{-1} = \ln\left(\frac{z_{0m}}{z_{0h}}\right). \tag{10}$$

c. Determination of bulk transfer coefficient

The bulk transfer coefficients C_D and C_H are not only important for indicating the intensity of turbulent transfer but are also necessary for dealing with some theoretical and practical problems, such as energy budget computation, diagnostic weather analysis, and numerical simulation for the atmospheric circulation or climate (Li et al. 2001). It is very important in theory and practice to study the value and variation of the bulk transfer coefficients over the Tibetan Plateau. The most popular approach to determine bulk transfer coefficients is to use profile relationships established from surface layer similarity and to express them as functions of surface roughness and Monin–Obukhov stability parameter (Li et al. 2001). The momentum bulk transfer coefficients and heat bulk transfer coefficients can be parameterized as (Garratt 1992)

$$C_D = \frac{\kappa^2}{[\ln(z/z_{0m}) - \psi_m(z/L, z_{0m}/L)]^2} \quad \text{and} \tag{11}$$

$$C_H = \frac{\kappa^2}{\mathrm{Pr}_0[\ln(z/z_{0m}) - \psi_m(z/L, z_{0m}/L)][\ln(z/z_{0m}) - \psi_h(z/L, z_{0h}/L)]}, \tag{12}$$

where $\psi_m(\zeta)$ is the integrated form of the stability function for momentum and $\psi_h(\zeta)$ is the integrated form of the stability function for heat. The z is the height above the zero-plane displacement, and L is the Monin–Obukhov

TABLE 3. Average KB^{-1} of the three stations: Qomolangma (Qomo.), Nam Co, and Southeast Tibet (South. T.).

Station	Jan	Feb	Mar	Apr	May	Jun	Jul	Aug	Sep	Oct	Nov	Dec
Qomo.	4.98	4.19	4.14	4.21	4.54	3.67	3.51	3.56	3.23	3.65	3.59	4.42
Nam Co	4.69	4.29	3.80	3.78	—	4.51	—	3.04	2.86	3.00	2.48	4.3
South. T.	5.86	5.88	6.00	6.87	7.86	8.06	7.07	6.47	6.47	6.29	7.13	7.81

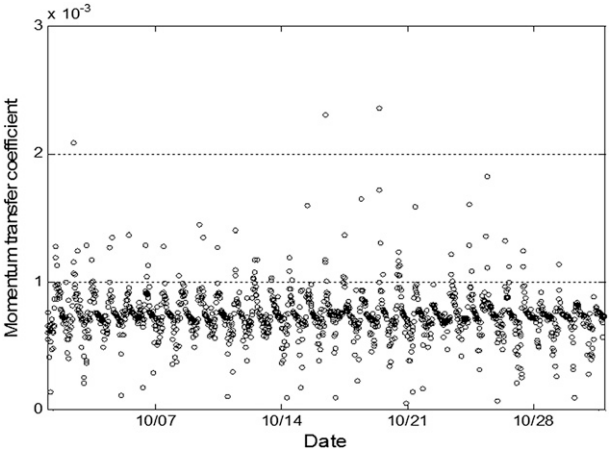

FIG. 6. The diurnal variations of momentum transfer coefficient (C_D) at Qomolangma in October.

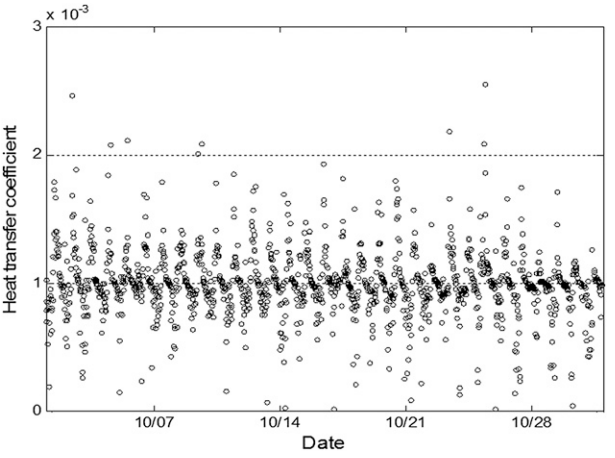

FIG. 7. As in Fig. 6, but for the heat transfer coefficient (C_H).

length; z_{0m} is the aerodynamic roughness length and z_{0h} is the thermal roughness length. The k is von Kármán's constant, and Pr_0 (=0.74) is the turbulent Prandtl number for neutral stability.

4. Analysis of the results

Figure 2 shows the frequency distribution of $\ln(z_{0m})$ at Nam Co in October. A value of $\ln(z_{0m}) = -4.78$ has the maximum frequency in the smoothed curve, and therefore the optimal value of z_{0m} is 0.0084 m. Covered with snow, the surface of the site became more smooth at that time of year. The monthly average z_{0m} for the whole year of 2007 is derived, and it is shown in Table 2. The intermonthly variations of aerodynamic roughness length at Nam Co and the Southeast Tibet station are more evident than that at Qomolangma.

The parameter kB^{-1} exhibits clear diurnal variations with lower values in the night and higher values in the daytime, especially in the afternoon at all three stations (see Figs. 3–5). Negative values of kB^{-1} are often observed in the night for relatively smooth surfaces on the Tibetan Plateau. Negative kB^{-1} values were also reported by previous studies (e.g., Verhoef et al. 1997; Su et al. 2001; Yang et al. 2008). This finding indicates that heat transfer efficiency may exceed that of momentum transfer (Yang et al. 2008). This is in contrast to the traditional opinion that momentum transfer is more efficient than heat transfer. Yang et al. (2008) reported that the ''abnormal'' phenomenon may be attributed to heat transport by inactive eddies in the outer layer. Possibly, negative values of kB^{-1} result from overestimation of downward heat flux in the night. We have to mention that negative kB^{-1} values might relate to the breakdown of Monin–Obukhov similarity when the thermal stratification is very stable. Figure 3 shows the diurnal variations of observed kB^{-1} at Qomolangma from 1 to 15 March. Figure 4 and Fig. 5 show the variations of observed kB^{-1} at Nam Co and Southeast Tibet station from 1 to 15 March, respectively. Table 3 illustrates intermonthly variations of kB^{-1} for all three stations. It can be seen that kB^{-1} at Southeast Tibet station is a little larger.

Figure 6 and Fig. 7 show the diurnal variations of the momentum transfer and heat transfer coefficients at Qomolangma, respectively. The average value of momentum transfer coefficient at Qomolangma in October is 0.73×10^{-3}, while that of heat transfer coefficient is 1×10^{-3}. Table 4 is the average momentum bulk transfer coefficients of the whole year, and Table 5 is the average heat bulk transfer coefficients. The values of average heat bulk transfer coefficients are larger than those of average momentum bulk transfer

TABLE 4. The average momentum transfer coefficient ($\times 10^{-3}$) of the three stations: Qomolangma (Qomo.), Nam Co, and Southeast Tibet (South. T.).

Station	Jan	Feb	Mar	Apr	May	Jun	Jul	Aug	Sep	Oct	Nov	Dec
Qomo.	0.65	0.75	0.65	0.82	0.92	0.79	0.67	0.72	0.74	0.76	0.65	0.65
Nam Co	0.53	0.68	0.60	0.68	—	0.81	—	0.64	0.49	0.43	0.42	0.43
South. T.	1.2	1.2	1.3	2.9	6.6	5.4	4.1	2.8	2.7	3.0	3.8	4.1

TABLE 5. The average heat transfer coefficient ($\times 10^{-3}$) of the three stations: Qomolangma (Qomo.), Nam Co, and Southeast Tibet (South. T.).

Station	Jan	Feb	Mar	Apr	May	Jun	Jul	Aug	Sep	Oct	Nov	Dec
Qomo.	0.89	1.1	0.90	1.2	1.4	1.2	0.94	1.0	1.0	1.1	0.90	0.91
Nam Co	0.73	1.0	0.82	0.94	—	1.1	—	0.89	0.67	0.58	0.58	0.58
South. T.	1.8	1.9	1.9	4.8	9.8	8.0	6.6	4.6	4.4	4.5	5.8	5.9

coefficients on the Tibetan Plateau, which was also reported by previous studies (e.g., Miao et al. 1998; Li et al. 2002).

5. Conclusions and remarks

The variation of momentum transfer coefficient (C_D), heat transfer coefficient (C_H), aerodynamic roughness length (z_{0m}), thermal roughness length (z_{0h}), and excess resistance to heat transfer (kB^{-1}) at three stations on the Tibetan Plateau are analyzed in this study. The intermonthly variations of aerodynamic roughness length at Nam Co and the Southeast Tibet station are more evident than those at Qomolangma. The values of average heat bulk transfer coefficients C_D are larger than those of average momentum bulk transfer coefficients C_H. The parameter kB^{-1} exhibits clear diurnal variations with lower values in the night and higher values in the daytime, especially in the afternoon. Negative values of kB^{-1} are often observed in the night for relatively smooth surfaces on the Tibetan Plateau, indicating that heat transfer efficiency may exceed that of momentum transfer. This is in contrast to the traditional opinion that momentum transfer is more efficient than heat transfer. We suspect that negative kB^{-1} values might relate to very stable stratification where Monin–Obukhov similarity does not hold.

In fact, these parameters are quite changeable even over only over a few days. What is more, they vary with atmospheric stability and the upwind area where the atmospheric flux is measured. Thus, further study is necessary, including applying footprint models to assess flux data quality for these sites with respect to both fetch (the length of the homogeneous surface in the direction of wind) and surface homogeneity.

Acknowledgments. This work was under the auspices of the Chinese National Key Programme for Developing Basic Sciences (2010CB951701), the National Natural Science Foundation of China (40825015 and 40810059006), Innovation Projects of the Chinese Academy of Sciences (KZCX2-YW-Q11-01), and EU-FP7 project ''CEOP-AEGIS'' (212921). The authors thank all the colleagues for their very hard work in the construction and the field work of the Tibetan Observation and Research Platform (TORP).

REFERENCES

Beljaars, A. C. M., and A. A. M. Holtslag, 1991: Flux parameterization over land surfaces for atmospheric models. *J. Appl. Meteor.,* **30,** 327–341.

Brutsaert, W. H., 1982: *Evaporation into the Atmosphere: Theory, History, and Applications*. D. Reidel, 299 pp.

Garratt, J. R., 1992: *The Atmospheric Boundary Layer*. Cambridge University Press, 316 pp.

——, and R. J. Francey, 1978: Bulk characteristics of heat transfer in the unstable, baroclinic atmospheric boundary layer. *Bound.-Layer Meteor.,* **15,** 399–421.

Högström, U., 1996: Review of some basic characteristics of the atmospheric surface layer. *Bound.-Layer Meteor.,* **78,** 215–246.

Kaimal, J. C., and J. J. Finnigan, 1994: *Atmospheric Boundary Layer Flows: Their Structure and Measurement*. Oxford University Press, 289 pp.

Kanda, M., M. Kanega, T. Kawai, R. Moriwaki, and H. Sugawara, 2007: Roughness lengths for momentum and heat derived from outdoor urban scale models. *J. Appl. Meteor. Climatol.,* **46,** 1067–1079.

Li, G., and H. Tao, 2005: Characteristics of bulk transfer coefficient in precipitation processes of Tibetan plateau. *Plateau Meteor.,* **24,** 577–584.

——, T. Duan, S. Haginoya, and L. Chen, 2001: Estimates of the bulk transfer coefficients and surface fluxes over the Tibetan Plateau using AWS data. *J. Meteor. Soc. Japan,* **79,** 625–635.

——, B. Zhao, and J. Lu, 2002: Characteristics of bulk transfer coefficient over the Tibetan Plateau. *Acta Meteor. Sin.,* **60,** 60–66.

Ma, Y., O. Tsukamoto, J. Wang, H. Ishikawa, and I. Tamagawa, 2002: Analysis of aerodynamic and thermodynamic parameters on the grassy marshland surface of Tibetan Plateau. *Prog. Nat. Sci.,* **12,** 36–40.

——, M. Menenti, R. Feddes, and J. Wang, 2008: Analysis of the land surface heterogeneity and its impact on atmospheric variables and the aerodynamic and thermodynamic roughness lengths. *J. Geophys. Res.,* **113,** D08113, doi:10.1029/2007JD009124.

Miao, M., H. Cao, and J. Ji, 1998: Analysis of turbulent characteristics in atmospheric boundary layer over the Qinghai-Xizang Plateau. *Plateau Meteor.,* **17,** 356–363.

Owen, P. R., and W. R. Thomson, 1963: Heat transfer across rough surfaces. *J. Fluid Mech.,* **15,** 321–334.

Paulson, C. A., 1970: The mathematical representation of wind speed and temperature profiles in the unstable atmospheric surface layer. *J. Appl. Meteor.,* **9,** 857–861.

Sheppard, P. A., 1958: Transfer across the earth's surface and through the air above. *Quart. J. Roy. Meteor. Soc.,* **84,** 205–224.

Su, Z., T. Schmugge, W. P. Kustas, and W. J. Massman, 2001: An evaluation of two models for estimation of roughness height for heat transfer between the land surface and the atmosphere. *J. Appl. Meteor.,* **40,** 1933–1951.

Verhoef, A., H. A. R. De Bruin, and B. J. J. M. Van Den Hurk, 1997: Some practical notes on the parameter kB^{-1} for sparse vegetation. *J. Appl. Meteor.,* **36,** 560–572.

Webb, E. K., G. I. Pearman, and R. Leuning, 1980: Correction of flux measurements for density effects due to heat and water vapour transfer. *Quart. J. Roy. Meteor. Soc.,* **106,** 85–100.

Wilczak, J. M., S. P. Oncley, and S. A. Stage, 2001: Sonic anemometer tilt correction algorithms. *Bound.-Layer Meteor.,* **99,** 127–150.

Yang, K., N. Tamai, and T. Koike, 2001: Analytical solution of surface layer similarity equations. *J. Appl. Meteor.,* **40,** 1647–1653.

——, T. Koike, H. Fujii, K. Tamagwa, and N. Hirose, 2002: Improvement of surface flux parameterizations with a turbulence-related length. *Quart. J. Roy. Meteor. Soc.,* **128,** 2073–2087.

——, ——, and D. Yang, 2003: Surface flux parameterization in the Tibetan Plateau. *Bound.-Layer Meteor.,* **106,** 245–262.

——, and Coauthors, 2007: Auto-calibration system developed to assimilate AMSR-E data into a land surface mode for estimating soil moisture and the surface energy budget. *J. Meteor. Soc. Japan,* **85,** 229–242.

——, and Coauthors, 2008: Turbulent flux transfer over bare-soil surfaces: Characteristics and parameterization. *J. Appl. Meteor. Climatol.,* **47,** 276–290.

Zeng, X., and R. E. Dickinson, 1998: Effect of surface sublayer on surface skin temperature and fluxes. *J. Climate,* **11,** 537–550.